

*ARMY RESEARCH LABORATORY*



# **Nanomagnetics-magnetic Nanoparticles Filled Carbon Nanotubes**

**by Dereje Seifu, Govind Mallick, and Shashi P. Karna**

---

**ARL-TR-5957**

**March 2012**

## **NOTICES**

### **Disclaimers**

The findings in this report are not to be construed as an official Department of the Army position unless so designated by other authorized documents.

Citation of manufacturer's or trade names does not constitute an official endorsement or approval of the use thereof.

Destroy this report when it is no longer needed. Do not return it to the originator.

# **Army Research Laboratory**

Aberdeen Proving Ground MD 21005-5069

---

---

**ARL-TR-5957**

**March 2012**

---

---

## **Nanomagnetics-magnetic Nanoparticles Filled Carbon Nanotubes**

**Dereje Seifu**

**Morgan State University, Baltimore, MD 21251**

**Govind Mallick**

**Vehicle Technology Directorate, ARL**

**Shashi P. Karna**

**Weapons and Materials Research Directorate, ARL**

| REPORT DOCUMENTATION PAGE   |                             |                              | Form Approved<br>OMB No. 0704-0188                         |  |   |
|---|-----------------------------|------------------------------|--|--|---|
| Public reporting burden for this collection of information is estimated to average 1 hour per response, including the time for reviewing instructions, searching existing data sources, gathering and maintaining the data needed, and completing and reviewing the collection information. Send comments regarding this burden estimate or any other aspect of this collection of information, including suggestions for reducing the burden, to Department of Defense, Washington Headquarters Services, Directorate for Information Operations and Reports (0704-0188), 1215 Jefferson Davis Highway, Suite 1204, Arlington, VA 22202-4302. Respondents should be aware that notwithstanding any other provision of law, no person shall be subject to any penalty for failing to comply with a collection of information if it does not display a currently valid OMB control number.<br><b>PLEASE DO NOT RETURN YOUR FORM TO THE ABOVE ADDRESS.</b>  |                             |                              |  |  |   |
| 1. REPORT DATE (DD-MM-YYYY)<br>March 2012   |                             | 2. REPORT TYPE<br>Final      |  | 3. DATES COVERED (From - To)<br>01 September 2008 to 30 September 2012 |   |
| 4. TITLE AND SUBTITLE<br>Nanomagnetics–metallic Nanoparticles Filled Carbon Nanotubes   |                             |                              | 5a. CONTRACT NUMBER<br>W911QX-08-C-0102                    |  |   |
|   |                             |                              | 5b. GRANT NUMBER   |  |   |
|   |                             |                              | 5c. PROGRAM ELEMENT NUMBER                                 |  |   |
| 6. AUTHOR(S)<br>Dereje Seifu, Govind Mallick, and Shashi P. Karna   |                             |                              | 5d. PROJECT NUMBER   |  |   |
|   |                             |                              | 5e. TASK NUMBER  |  |   |
|   |                             |                              | 5f. WORK UNIT NUMBER                                       |  |   |
| 7. PERFORMING ORGANIZATION NAME(S) AND ADDRESS(ES)<br>U.S. Army Research Laboratory<br>ATTN: RDRL-VTM<br>Aberdeen Proving Ground MD 21005-5069  |                             |                              | 8. PERFORMING ORGANIZATION<br>REPORT NUMBER<br>ARL-TR-5957 |  |   |
| 9. SPONSORING/MONITORING AGENCY NAME(S) AND ADDRESS(ES)   |                             |                              | 10. SPONSOR/MONITOR'S ACRONYM(S)                           |  |   |
|   |                             |                              | 11. SPONSOR/MONITOR'S REPORT<br>NUMBER(S)                  |  |   |
| 12. DISTRIBUTION/AVAILABILITY STATEMENT<br>Approved for public release; distribution unlimited.   |                             |                              |  |  |   |
| 13. SUPPLEMENTARY NOTES   |                             |                              |  |  |   |
| 14. ABSTRACT<br>The high demand for nanoelectronics devices, high density magnetic memories, sensors, and energy storage for the future force and warfighters have led us to develop unique methods to fill vertically aligned nanofibers with magnetic nanoparticles such as cobalt ferrite (CoFe <sub>2</sub> O <sub>4</sub> ), iron (Fe), and nickel cobalt (NiCo). In this work, pulsed laser deposition (PLD) is used to fill CoFe <sub>2</sub> O <sub>4</sub> and DC magnetron sputtering is used to fill Fe and NiCo in carbon nanotubes (CNTs). The filled CNTs are characterized by scanning electron microscopy (SEM), energy-dispersive spectrometry (EDS), atomic force microscopy (AFM), magnetic force microscopy (MFM), and vibrating sample magnetometer (VSM). Magnetization measurements in-plane and out-of-plane with respect to the sample's surface of CNTs filled with CoFe <sub>2</sub> O <sub>4</sub> indicates a reasonable coercivity of 0.4 T. The magnetic anisotropy is, however, found out to be randomly oriented indicating a polycrystalline structure. The unique difference between the in-plane and out-of-plane magnetizations is the sharing produced by the demagnetizing field in the perpendicular direction. |                             |                              |  |  |   |
| 15. SUBJECT TERMS<br>CNTs, EDX, AFM, STM, MFM, SEM, VSM   |                             |                              |  |  |   |
| 16. SECURITY CLASSIFICATION OF:   |                             |                              | 17. LIMITATION<br>OF<br>ABSTRACT<br>UU                     | 18. NUMBER<br>OF<br>PAGES<br>24  | 19a. NAME OF RESPONSIBLE PERSON<br>Govind Mallick           |
| a. REPORT<br>Unclassified   | b. ABSTRACT<br>Unclassified | c. THIS PAGE<br>Unclassified |  |  | 19b. TELEPHONE NUMBER (Include area code)<br>(410) 278-2050 |

---

## Contents

---

|   |           |
|---|-----------|
| <b>List of Figures</b>                              | <b>iv</b> |
| <b>Acknowledgment</b>                               | <b>v</b>  |
| <b>1. Introduction and Background</b>               | <b>1</b>  |
| <b>2. Materials and Methods</b>                     | <b>3</b>  |
| <b>3. Results and Discussions</b>                   | <b>4</b>  |
| <b>4. Conclusions</b>                               | <b>9</b>  |
| <b>5. References</b>                                | <b>10</b> |
| <b>List of Symbols, Abbreviations, and Acronyms</b> | <b>13</b> |
| <b>Distribution List</b>                            | <b>15</b> |

---

## List of Figures

---

|   |   |
|---|---|
| Figure 1. SEM of vertically grown MWCNTs on SiO <sub>2</sub> .....  | 4 |
| Figure 2. SEM of vertically grown MWCNTs on SiO <sub>2</sub> filled with CoFe <sub>2</sub> O <sub>4</sub> by PLD at high resolution (a) and lower resolution (b).....   | 5 |
| Figure 3. Magnetic moment vs. applied field; the solid line represent in-plane and the scatter line represents out-of-plane magnetization. ....   | 5 |
| Figure 4. SEM of vertically grown MWCNTs on SiO <sub>2</sub> filled with Fe by DC magnetron sputtering at 0° from the normal of the substrate in (a) and at 70° from the normal (b). ....   | 6 |
| Figure 5. Magnetic moment vs. applied field; the solid line represent in plane and scatter represent out of plane magnetization of vertically grown MWCNTs on SiO <sub>2</sub> filled with Fe by DC magnetron sputtering at 0° from the normal of the substrate in (a) and at 70° from the normal (b). .... | 7 |
| Figure 6. (a) AFM scan of MWCNTs filled with Fe sputtered head-on and (b) the corresponding MFM scan. ....  | 8 |
| Figure 7. MFM scan of MWCNTs filled with Fe sputtered head-on. ....   | 8 |
| Figure 8. 3-D AFM scan of MWCNTs filled with Fe sputtered head-on.....  | 8 |

---

## **Acknowledgment**

---

This work was supported by the U.S. Army Research Laboratory through the contract number W911QX-08-C-0102. We would like to thank Professor P. M. Ajayan at Rice University, Department of Mechanical Engineering & Materials Science, Houston, TX, and Dr. M. Meyyappan, Director and Senior Scientist at Ames' Center for Nanotechnology in Moffett Field, CA, for supplying vertically grown carbon nanotubes (CNTs). This work was also supported in part by NSF-MRI-R2 grant (Award No. 0958950).

INTENTIONALLY LEFT BLANK.

---

## 1. Introduction and Background

---

Since the first comprehensive and detailed characterization of carbon nanotubes (CNTs) by Iijima in 1991 (1), the saga to fill the low-dimensional space inside CNTs with different types of applications-related materials has continued. Pristine CNTs possess incredible mechanical and electrical properties (2, 3) besides the hallowed enclosed volume of space. This low-dimensional space provides an excellent opportunity to enhance the property of CNTs by filling it with applications-related materials (4). A few examples include improved photovoltaic performance demonstrated in platinum (Pt)-filled CNTs (5) and the possibility of lightweight wide-band microwave absorbers using ferromagnetic-filled CNTs (6). CNTs filled with magnetic nanoparticles are attractive candidates for active elements in changeable diffraction gratings, filters, and polarizer (7).

Filling CNTs with both ferromagnetic and ferroelectric materials could be another way of coupling the two properties, hence fabricating multi-ferroic materials (8, 9). Iodine-filled CNTs have shown high electrical conductivity and excellent mechanical property (10). Molecular dynamic simulations (11–13) indicate improved mechanical behavior of filled CNTs compared to unfilled CNTs. Increased compressibility of iron (Fe)-filled CNTs has been observed with high-pressure x-ray diffraction (14). The mechanical strength of filled CNTs and their buckling behavior make them ideal for use as tips for scanning probe microscopes (15). CNTs filled with indium (In) can be used as nanoscale mass conveyers in a nano assembly tool (16).

When filling CNTs with conductive fluids, a voltage is generated between the tube ends indicating potential application of CNTs in flow sensing and converting mechanical energy to an electrical signal (17). Silver-filled CNTs are promising to be used as spectroscopic enhancers and chemical sensors in the visible range (18). Filling CNTs with hydrogen has application for mobile energy storage at room temperature (19).

The list of applications of nanotubes filled with magnetic material also includes materials for wearable electronics (20), cantilever tips in magnetic force microscope (21), magnetic stirrers in microfluidic devices, and magnetic valves in nanofluidic devices. Biomedical applications include capsules or nanosubmarines for magnetically guided drug delivery to desired locations in the body, and non-pervasive diagnosis and treatment that can bypass surgery (22).

Nanomagnets are also important from a fundamental point of view in understanding the physics of one-dimensional magnets. The low-dimensional enclosed space of CNTs offer an environment in which previously unknown physical phenomena at nanoscale level can be observed. For example, confinement of matter on the nanoscale can induce phase transitions not seen in bulk systems (23–27). It can also be used as a template to synthesize nanowires and nanomagnets.

The major hurdle for applications-related filling is the assembly of ordered nanoscale structures and controlled fillings. There has been success in preparing aligned nanotubes vertically on silicon dioxide ( $\text{SiO}_2$ ) substrate by chemical vapor deposition (CVD) technique (28). In this work we report a single step procedure used to fill vertically aligned multi-walled (MW) CNTs with cobalt ferrite ( $\text{CoFe}_2\text{O}_4$ ) using pulsed laser deposition (PLD) and with Fe using sputtering. This is the first attempt ever to fill CNTs using PLD (29) and magnetron sputtering (30, 31), which are the two commonly used techniques to prepare various applications related thin and thick films.

PLD is a type of physical vapor deposition (PVD) technique where a high power pulse laser beam is focused inside a vacuum chamber to strike a target of the material that is to be deposited. Thus, the material is vaporized from the target (in a plasma plume), which deposits itself as a thin film on a substrate (such as a silicon wafer facing the target). The removal of atoms from the bulk material is done by vaporization of the bulk at the surface region in a state of non-equilibrium. In this, the incident laser pulse penetrates into the surface of the material within the penetration depth. This dimension is dependent on the laser wavelength and the index of refraction of the target material at the applied laser wavelength (248 nm). The strong electrical field generated by the laser light is sufficiently strong to remove the electrons from the bulk material of the penetrated volume. The free electrons oscillate within the electromagnetic field of the laser light and can collide with the atoms of the bulk material, thus transferring some of their energy to the lattice of the target material within the surface region. The surface of the target is then heated up and the material is vaporized. In the second stage, the material expands in plasma parallel to the normal vector of the target surface towards the substrate due to Coulomb repulsion and recoils from the target surface. The spatial distribution of the plume is dependent on the background pressure inside the PLD chamber. PLD is only one of many thin-film deposition techniques. Other methods include sputter deposition (radio frequency [RF], magnetron, and ion beam).

Sputter deposition is also based on PVD in which materials are sputtered on a substrate from a target. Sputtered atoms ejected from the target have a wide energy distribution, typically up to tens of eV. The sputtered ions are ballistic from the target in straight lines and impact energetically on the substrates or vacuum chamber causing re-sputtering. Alternatively, at higher gas pressures, the ions collide with the gas atoms that act as a moderator and move diffusively, reaching the substrates or vacuum chamber wall and condensing after undergoing a random walk. The entire range from high-energy ballistic impact to low-energy thermal motion is accessible by changing the background gas pressure. The sputtering gas is often an inert gas such as argon. For efficient momentum transfer, the atomic weight of the sputtering gas should be close to the atomic weight of the target, so for sputtering light elements neon is preferable, while for heavy elements krypton or xenon are used. Reactive gases can also be used to sputter compounds. The compound can be formed on the target surface, in-flight or on the substrate depending on the process parameters. The availability of many parameters that control sputter

deposition makes it a complex process, but also allows experts a large degree of control over the growth and microstructure of the film. An important advantage of sputter deposition is that even materials with very high melting points are easily sputtered. Sputtering sources are usually magnetrons that use strong electric and magnetic fields to trap electrons close to the surface of the magnetron, which is known as the target. The electrons follow helical paths around the magnetic field lines undergoing more ionizing collisions with gaseous neutrals near the target surface than would otherwise occur. The extra ions created as a result of these collisions lead to a higher deposition rate. It also means that the plasma can be sustained at a lower pressure. The sputtered atoms are neutrally charged, and hence, unaffected by the magnetic trap. Though, there have been previous attempts (32) to fill multi-walled carbon nanotubes (MWCNTs) in aqueous suspension with  $\text{CoFe}_2\text{O}_4$ , the methods presented in this work are more functionally oriented as the tubes are aligned and possess high symmetry.

---

## 2. Materials and Methods

---

The vertically aligned MWCNTs used in this filling experiment are grown using a thermal CVD method (28) on a  $\text{SiO}_2$  substrate. This method involves exposing silica structures to a mixture of ferrocene and xylene at  $770^\circ\text{C}$  for 10 min. The furnace is pumped down to  $\sim 200$  mTorr in argon bleed and then heated to the temperature of  $770^\circ\text{C}$ . The solution of ferrocene dissolved in xylene ( $\sim 0.01\text{g/ml}$ ) is pre-heated in a bubbler to  $175^\circ\text{C}$  and then passed through the tube furnace. The furnace is then cooled down to room temperature. The open ended MWCNTs tips are filled with  $\text{CoFe}_2\text{O}_4$  using PLD and with Fe and nickel cobalt (NiCo) using DC magnetron sputtering methods.

$\text{CoFe}_2\text{O}_4$  is used in this work due to its high anisotropy ( $4 \times 10^6$  ergs/cm<sup>2</sup>) and magnetostriction ( $800 \times 10^{-6}$ ) at room temperature (33). The target  $\text{CoFe}_2\text{O}_4$  for laser ablation is prepared using the combination of ferric and cobalt oxides in a 2:1 ratio, respectively (34). The polycrystalline  $\text{CoFe}_2\text{O}_4$  filling in MWCNT is carried out in a high vacuum ( $2 \times 10^{-7}$  Torr) with a 100-W pulsed excimer laser (krypton fluoride [KrF]) at  $1.5\text{ J/cm}^2$  and 3 Hz as the energy density and repetition rate at a 248-nm wavelength, respectively. During deposition, the  $\text{SiO}_2$  template is heated at  $300^\circ\text{C}$  and the target is rotated in order to ensure its uniform wear. A total of 12,000 shots are fired to fill the nanotubes at 3 Hz in an oxygen pressure of 30 mTorr with output energy of 800 mJ.

DC magnetron sputtering is used to fill vertically aligned MWCNTs with NiCo and Fe. A gun power of 50 W and an argon pressure of 0.07 Torr are maintained during the 30-min deposition. Then, 51 nm of the sputtering material is deposited over the CNTs at the deposition rate of  $1.7\text{ \AA/s}$ . Deposition is carried out at an angle of  $0^\circ$  from the normal to the substrate surface. A second sample at an angle of  $70^\circ$  from the normal is also prepared. The latter deposition at  $70^\circ$  is an oblique deposition known for constructing nanocolumns. When deposition angle with the

substrate normal is high, a columnar structure is observed (35). The unique structure consisting of separated columns inclined toward the deposition direction is due to the “shadowing effect,” which is caused by the height of the initial nuclei. A shadow is formed behind the initial nuclei where the rest of the vapor flux cannot reach. Since the surface mobility of the deposited adatoms is low at room temperature the growth rate in the normal to the surface is higher than that in the plane.

---

### 3. Results and Discussions

---

Scanning electron microscopy (SEM) of vertically aligned MWCNTs grown on a  $\text{SiO}_2$  substrate before deposition is depicted in figure 1. As shown in the figure, most of the tubes are aligned vertically and only very few are misaligned. Filling by PLD method is mediated by the highly energetic particles in the plasma formed when an excimer laser of KrF of average power (100 W) and a wavelength of 248 nm strike the target material, i.e.,  $\text{CoFe}_2\text{O}_4$ . Due to the high energy, in the order of several hundreds of eV's, the particles penetrate deep into the lumen of the CNTs. However, these highly energetic particles also increase the probability to damage the CNT openings by colliding with the edges. At present, the only mechanism to control this from occurring results in slowing all the particles by increasing background pressure. This has a negative consequence, however. The particles do not have enough momentum to travel deep into the lumen of the CNT. In this work, 30 mTorr of background oxygen pressure is applied to prevent  $\text{CoFe}_2\text{O}_4$  particles from colliding with the edges of CNTs. Figure 2 depicts SEM of vertical tubes after being filled by PLD with  $\text{CoFe}_2\text{O}_4$ . From SEM measurements, it was not feasible to determine the filling depth; however, in single crystals, the depth can be determined using in- and out-of-plane magnetization measurements (36).

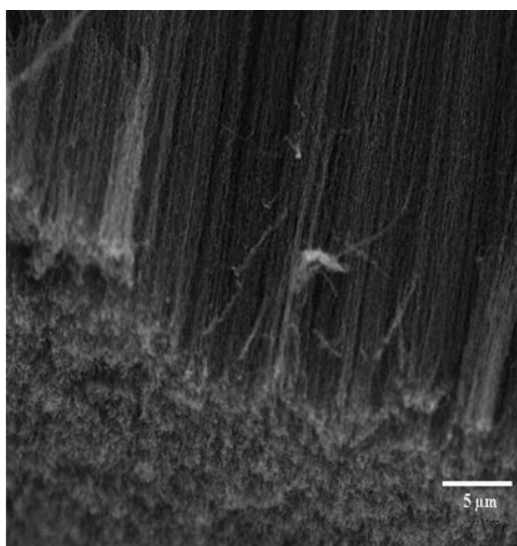


Figure 1. SEM of vertically grown MWCNTs on  $\text{SiO}_2$ .

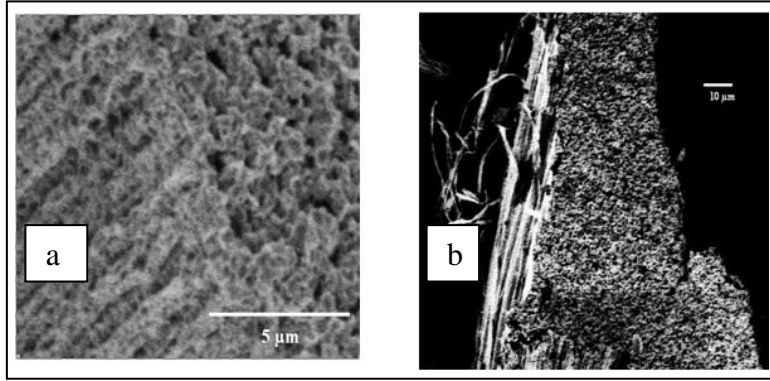


Figure 2. SEM of vertically grown MWCNTs on SiO<sub>2</sub> filled with CoFe<sub>2</sub>O<sub>4</sub> by PLD at high resolution (a) and lower resolution (b).

Magnetization measurements are performed using vibrating sample magnetometer (VSM) both in-plane and out-of-plane loops with respect to the sample's surface. Figure 3 shows the magnetic moments with respect to the applied fields for the two loops, indicating the high coercivity of 0.4 T. The high coercivity is due to the coupling of the spins of the cobalt (Co) ions to the Fe ions in the oxide structure.

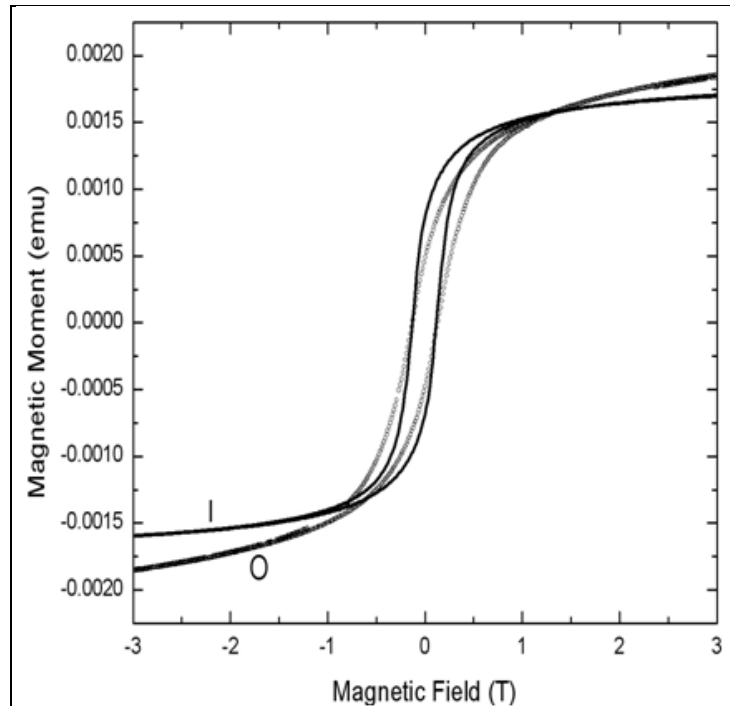


Figure 3. Magnetic moment vs. applied field; the solid line represent in-plane and the scatter line represents out-of-plane magnetization.

Magnetic properties of a material usually are very sensitive to its shape due to the dominating role of anisotropy in magnetism. In particular, the shape of the nanocrystals is a dominating factor for the coercivity. Such magnetic nanocrystals with distinct shapes possess tremendous potentials in technological applications of magnetic nanocrystals for high-density information

storage and also in the fundamental understanding of magnetism. The coercivity of nanoparticles from Stoner-Wohlfarth theory is determined by anisotropy constant and saturation magnetization (37):

$$H_C = 2K/(\mu_0 M_S), \quad (1)$$

where  $\mu_0$  is a universal constant of permeability in free space,  $K$  is the blocking temperature, and  $M_S$  is saturation magnetization.

The in-plane (solid line, figure 3) and out-of-plane (scattered line, figure 3) magnetization loops exhibit the same hysteresis. The in-plane and out-of-plane hysteresis curves coincide, indicating a high coupling between the in-plane and out-of plane anisotropy. The slight difference between the in-plane and out-of-plane magnetizations is the sharing produced by the demagnetizing field in the perpendicular direction.

Figure 4 shows the SEM and energy dispersive spectroscopy (EDS) of vertically grown MWCNTs filled by DC magnetron sputtering with Fe. In figure 4a, the deposition is parallel to the normal of the substrate surface and in figure 4b the deposition is oblique at an angle of  $70^\circ$  to the normal of the substrate surface. The EDS measurements show Fe peak and silicon (Si) peak which is due to the  $\text{SiO}_2$  substrate on which the CNTs are grown.

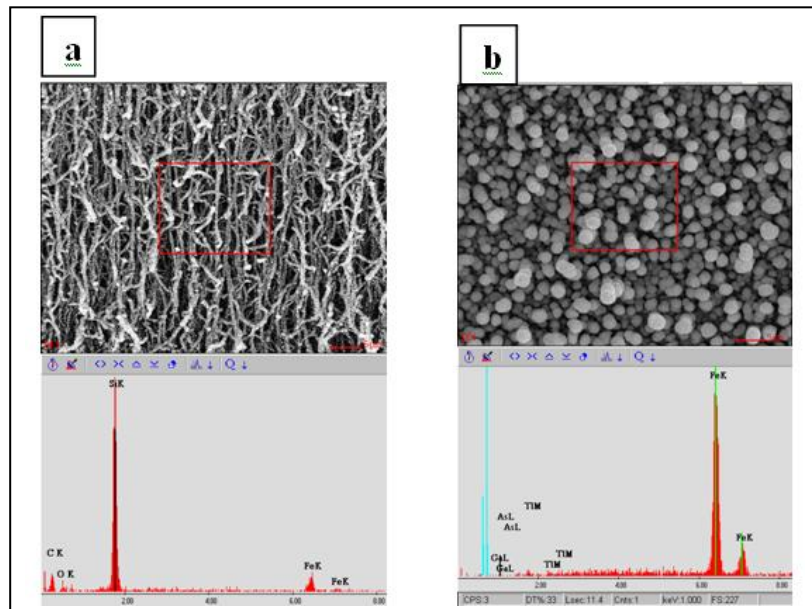


Figure 4. SEM of vertically grown MWCNTs on  $\text{SiO}_2$  filled with Fe by DC magnetron sputtering at  $0^\circ$  from the normal of the substrate in (a) and at  $70^\circ$  from the normal (b).

The graph of the magnetic moment of the Fe-filled MWCNTs as a function of applied field is shown in figure 5. Solid line represents in-plane and scatter represents out-of-plane magnetization. In both cases, the in-plane and out-of-plane magnetization hysteresis loops coincide, indicating a strong coupling between the in-plane and out-of-plane anisotropy, which is

mainly shape anisotropy due to the constricted spacing of the lumen of CNT. The hysteresis loop of Fe-filled MWCNT's deposited at  $0^\circ$  from the normal exhibits an anomalous narrowing of the loop at the zero magnetization axis. This anomalous hysteresis loop indicates somewhat indifferent domain behavior and is subject to further investigation.

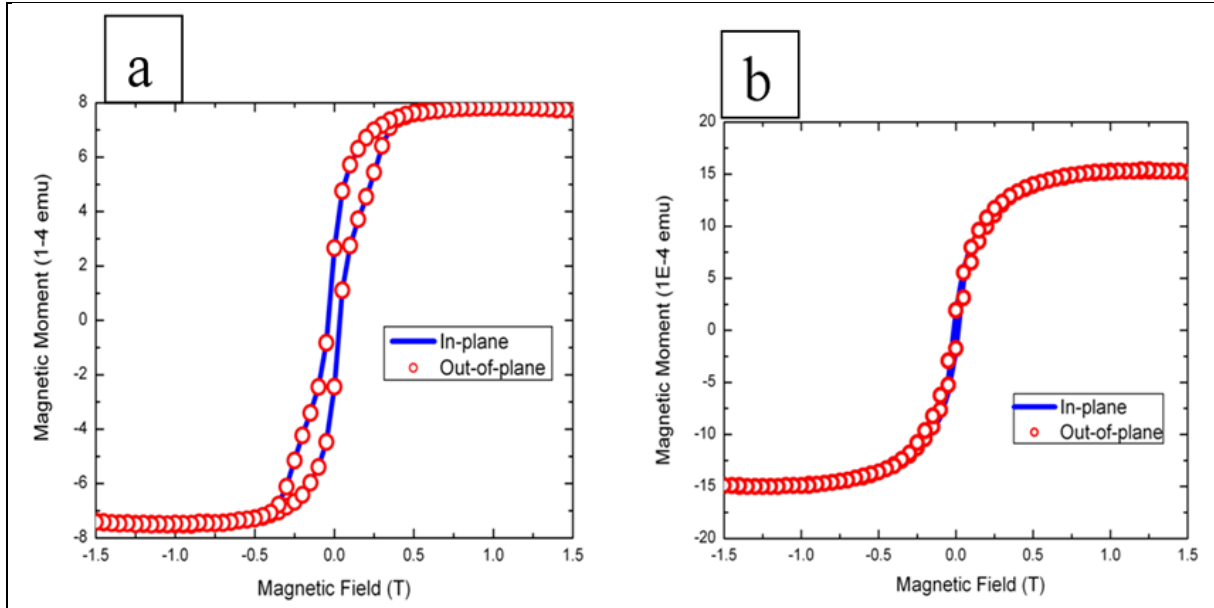


Figure 5. Magnetic moment vs. applied field; the solid line represent in plane and scatter represent out of plane magnetization of vertically grown MWCNTs on  $\text{SiO}_2$  filled with Fe by DC magnetron sputtering at  $0^\circ$  from the normal of the substrate in (a) and at  $70^\circ$  from the normal (b).

Figure 6 shows  $5 \times 5 \mu\text{m}^2$  scan areas of atomic force microscopy (AFM) and magnetic force microscopy (MFM) images of Fe-filled MWCNTs at the same spot of the sample prepared by DC magnetron sputtering. The distinct bright and dark regions in the MFM images have a greater length scale than the corresponding atomic force morphology images. The average domain size  $D$  is determined by measuring the distance between successive bright to dark regions using line scans across the MFM image. The competition between magnetostatic, exchange, magnetocrystalline, and any other growth-induced anisotropy energies lead to stripe domain configurations in which the domain size depends on the sample thickness and the domain configuration depends on the sample magnetic history. The theoretical explanation of the formation of magnetic domains is to minimize the magnetic energy of a ferromagnetic crystal.

Figures 7 and 8 illustrate two-dimensional (2-D) and three-dimensional (3-D) versions of the  $1.5 \times 1.5 \mu\text{m}^2$  scan area of magnified version of MFM image shown in figure 6b. The stripe domains in both figures are clearly visible with typical domain width thickness of  $0.25 \mu\text{m}$ .

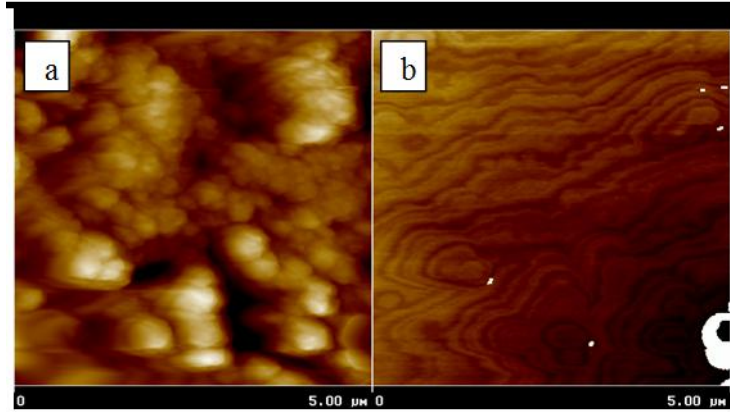


Figure 6. (a) AFM scan of MWCNTs filled with Fe sputtered head-on and (b) the corresponding MFM scan.

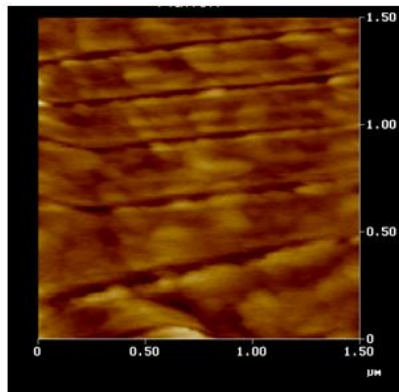


Figure 7. MFM scan of MWCNTs filled with Fe sputtered head-on.

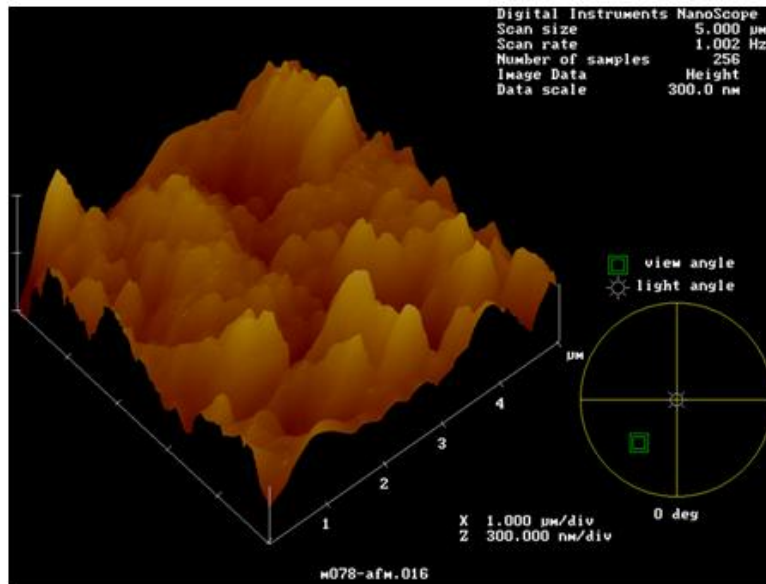


Figure 8. 3-D AFM scan of MWCNTs filled with Fe sputtered head-on.

---

## 4. Conclusions

---

In summary, for the first time, PLD technique and magnetron sputtering are used to fill vertically aligned CNTs with high-yield magnetic nanoparticles. The magnetization measurements suggest that the filled magnetic nanoparticles have a polycrystalline nature, as evidenced from the randomly oriented magnetic anisotropy.

Spin reorientation due to competition between shape anisotropy of nanotubes and magneto-crystalline component of anisotropy was observed while filling the MWCNTs with  $\text{CoFe}_2\text{O}_4$ , and seemed to be dependent on the lattice of the material.

The fillings of Fe and NiCo in the CNTs using magnetron sputtering method, showed an anomalous hysteresis in the VSM measurement and the stripe magnetic domains in the MFM measurement with an average thickness of  $0.25\ \mu\text{m}$ . This is indicative of a soft magnetic material.

We believe that our present work further extends the applications of CNT-based materials in nanoscale electronics technologies. This study opens up not only a simple and easy way preparation method and low-cost synthesis procedures, but also state-of-the-art industrial-scale preparation techniques. The fabrication of oxide nanowires using MWCNTs as templates will provide new approach to nanofabrication of ferromagnetic materials, high  $T_c$  superconductors, or colossal magnetoresistance (CMR) materials.

---

## 5. References

---

1. Iijima, S. Helical Microtubules of Graphitic Carbon, *Letters to Nature* **1991**, *354*, 56–58.
2. Osborne, I. S. A Nanotube Story with a Twist, *Science* **2003**, *302*, 749.
3. Tomblor, W. T.; Zhou, C.; Kong, J.; Dai, H. Gating Individual Nanotubes and Crosses with Scanning Probes. *Appl. Phys. Lett.* **2000**, *76*, 2412–2414.
4. Ivanovskaya, V. V.; Köhler, C.; Seifert, G. 3d Metal Nanowires and Clusters Inside Carbon Nanotubes: Structural, Electronic, and Magnetic Properties. *Phys. Rev. B* **2007**, *75*, 075410-7.
5. Somani, P. R.; Somani, S. P.; Umen, M. Application of Metal Nanoparticles Decorated Carbon Nanotubes in Photovoltaics. *Appl. Phys. Lett.* **2008**, *93*, 033315-3.
6. Lv, R.; Kang, F.; Gu, J.; Gui, X.; Wei, J.; Wang, K.; Wu, D. Carbon Nanotubes Filled with Ferromagnetic Alloy Nanowires: Lightweight and Wide-band Microwave Absorber. *Appl. Phys. Lett.* **2008**, *93*, 223105-3.
7. Kornev, K. G.; Halverson, D.; Korneva, G.; Gogotsi, Y.; Friedman, G. Magnetostatic Interactions Between Carbon Nanotubes Filled with Magnetic Nanoparticles *Appl. Phys. Lett.*, **2008**, *92*, 233117-3.
8. Zheng, H.; Wang, J.; Lofland, S. E.; Ma, Z.; Mohaddes-Ardabili, L.; Zhao, T.; Salamanca-Riba, L.; Shinde, S. R.; Ogale, S. B.; Bai, F.; Viehland, D.; Jia, Y.; Schlom, D. G.; Wuttig, M.; Roytburd, A.; Ramesh, R. Multiferroic BaTiO<sub>3</sub>-CoFe<sub>2</sub>O<sub>4</sub> Nanostructures. *Science* **2004**, *303*, 661–663.
9. Yang, C. K.; Zhao, J.; Lu, J. P. Magnetism of Transition-metal/Carbon-nanotube Hybrid Structures. *Phys. Rev. Lett.* **2003**, *90*, 257203-4.
10. Bin, Y.; Chen, Q.; Tashiro, K.; Matsuo, M. Electrical and Mechanical Properties of Iodine-Doped Highly Elongated Ultrahigh Molecular Weight Polyethylene Films with Multiwalled Carbon Nanotubes. *Phys. Rev. B* **2008**, *77*, 035419-7.
11. Jeong, B. W.; Lim, J. K.; Sinnott S. B. Tensile Mechanical behavior of Hollow and Filled Carbon Nanotubes Under Tension or Combined Tension-torsion. *Appl. Phys. Lett.* **2007**, *90*, 023102-3.
12. Wang, L.; Zhang, H. W.; Zhang, Z. Q.; Zheng, Y. G.; Wang, J. B. Buckling Behaviors of Single-walled Carbon Nanotubes Filled with Metal Atoms. *Appl. Phys. Lett.* **2007**, *91*, 051122-3.

13. Ni, B.; Sinnott, S. B.; Mikulski, P. T.; Harrison, J. A. Compression of Carbon Nanotubes Filled with  $C_{60}$ ,  $CH_4$ , or Ne: Predictions from Molecular Dynamics Simulations. *Phys. Rev. Lett.* **2002**, *88*, 205505-4.
14. Karmakar, S.; Sharma, S. M.; Teredesai, P. V.; Sood, A. K. Pressure-induced Phase Transitions in Iron-filled Carbon Nanotubes: X-ray Diffraction Studies. *Phys. Rev. B* **2004**, *69*, 165414-5.
15. Ye, Q.; Cassell, A. M.; Liu, H.; Chao, K. J.; Han, J.; Meyyappan, M. Large-scale Fabrication of Carbon Nanotube Probe Tips for Atomic Force Microscopy Critical Dimension Imaging Applications. *Nano Letters* **2004**, *4*, 1301–1308.
16. Regan, B. C.; Aloni, S.; Ritchie, R. O.; Dahmen, U.; Zettl, A. Carbon Nanotubes as Nanoscale Mass Conveyors. *Nature* **2004**, *428*, 924–927.
17. Ghosh, S.; Sood, A. K.; Kumar, N. Carbon Nanotube Flow Sensors. *Science* **2003**, *299*, 1042–1044.
18. García-Vidal, F. J.; Pitarke, J. M.; Pendry, J. B. Silver-filled Carbon Nanotubes Used as Spectroscopic Enhancers. *Phys. Rev. B* **1998**, *58*, 6783–6786.
19. Schlupbach, L.; Züttel, A. Hydrogen-storage Materials for Mobile Applications. *Nature* **2001**, *414*, 353–358.
20. Wu, Z.; Chen, Z.; Du, X.; Logan, J. M.; Sippel, J.; Nikolou, M.; Kamaras, K.; Reynolds, J. R.; Tanner, D. B.; Hebard, A. F.; Rinzler, A. G. Transparent, Conductive Carbon Nanotube Films. *Science* **2004**, *305*, 1273–1276.
21. Yoshida, N.; Arie, T.; Akita, S.; Nakayama, Y. Improvement of MFM Tips Using Fe-Alloy-Capped Carbon Nanotubes. *Physica B-Condens. Matter* **2002**, *323*, 149–150.
22. Alexiou, C.; Jurgons, R.; Seliger, C.; Iro, H. Medical Applications of Magnetic Nanoparticles. *J. of Nanoscience and Nanotech.* **2006**, *6* (9/10), 2762–2768.
23. Hummer, G.; Rasaiah, J. C.; Noworyta, J. P. Water Conduction through the Hydrophobic Channel of a Carbon Nanotube. *Nature* **2001**, *414*, 188–190.
24. Margine, E. R.; Lammert, P. E.; Crespi, V. H. Reciprocal Space Constraints Create Real-space Anomalies in Doped Carbon Nanotubes. *Phys. Rev. Lett.* **2007**, *99*, 196803-4.
25. Seifu, D.; Karna S. *Nanomagnetics*; ARL-TR-3790: U.S. Army Research Laboratory: Aberdeen Proving Ground, MD, April 2006.
26. Seifu, D.; Hijji, Y.; Hirsch, G.; Karna, S. Chemical Method of Filling Carbon Nanotubes with Magnetic Material. *Journal of Magnetism and Magnetic Materials* **2008**, *320* (3–4), 312–315.

27. Prados, C.; Crespo, P.; González, J. M.; Hernando, A.; Marco, J. F.; Gancedo, R.; Grobert, N.; Terrones, M.; Walton, R. M.; Kroto, H. W. Hysteresis Shift in Fe-filled Carbon Nanotubes due to  $\gamma$ -Fe. *Phys. Rev. B* **2002**, *65*, 113405-4.
28. Wei, B. Q.; Vajtai, R.; Jung, Y.; Ward, J.; Zhang, R.; Ramanath, G.; Ajayan, P. M. Assembly of Highly Organized Carbon Nanotube Architectures by Chemical Vapor Deposition. *Chem. Mater.* **2003**, *15*, 1598–1606.
29. Lowndes, D. H.; Geohegan, D. B.; Poretzky, A. A.; Norton, D. P.; Rouleau, C. M. Synthesis of Novel Thin-film Materials by Pulsed Laser Deposition. *Science* **1996**, *273*, 898–903.
30. Pitt, C. W. Thin Film Technology. *Nature* **1977**, *270*, 16.
31. Behrisch, R. *Sputtering by Particle bombardment* (ed.); Springer, Berlin, 1981.
32. Keller, N.; Pham-Huu, C.; Estournes, C.; Greneche, J.; Ehret, G.; Ledoux, M. Carbon Nanotubes as a Template for Mild Synthesis of Magnetic  $\text{CoFe}_2\text{O}_4$  Nanowires. *Carbon* **2004**, *42*, 1395–1399.
33. Bozorth, R. M.; Tilden, E. F.; Williams, A. J. Anisotropy and Magnetostriction of Some Ferrite. *Phys. Rev.* **1955**, *99*, 1788–1798.
34. Benjamin, J. S. Mechanical Alloying. *Sci. Am.* **1976**, *234*, 40.
35. Smith, D. L. *Thin Film Deposition – Principle and Practice*; McGraw-Hill, 1995.
36. Chikazumi, S. *Physics of Ferromagnetism*, 2<sup>nd</sup> ed., Clarendon Press., Oxford, 1977.
37. Stoner, E. C.; Wolfrath, E. P. A Mechanism of Magnetic Hysteresis in Heterogeneous Alloys. *Philos. Trans. R. Soc. London* **1948**, *Ser. A240*, 599.

---

## List of Symbols, Abbreviations, and Acronyms

---

|                                  |                                |
|----------------------------------|--------------------------------|
| 2-D                              | two-dimensional                |
| 3-D                              | three-dimensional              |
| AFM                              | atomic force microscopy        |
| CMR                              | colossal magnetoresistance     |
| CNT                              | carbon nanotube                |
| Co                               | cobalt                         |
| CoFe <sub>2</sub> O <sub>4</sub> | cobalt ferrite                 |
| CVD                              | chemical vapor deposition      |
| EDS                              | energy dispersive spectroscopy |
| Fe                               | iron                           |
| In                               | indium                         |
| KrF                              | krypton fluoride               |
| MFM                              | magnetic force microscopy      |
| MW                               | multi-walled                   |
| MWCNT                            | multi-wall carbon nanotube     |
| Ni                               | nickel                         |
| NiCo                             | nickel cobalt                  |
| PLD                              | pulsed laser deposition        |
| Pt                               | platinum                       |
| PVD                              | physical vapor deposition      |
| RF                               | radio frequency                |
| SEM                              | scanning electron microscopy   |
| Si                               | silicon                        |

SiO<sub>2</sub>

silicon dioxide

VSM

vibrating sample magnetometer

| NO. OF<br>COPIES | ORGANIZATION  |
|------------------|---|
| 1<br>ELEC        | ADMNSTR<br>DEFNS TECHL INFO CTR<br>ATTN DTIC OCP<br>8725 JOHN J KINGMAN RD STE 0944<br>FT BELVOIR VA 22060-6218   |
| 1                | US ARMY RSRCH DEV AND ENGRG<br>CMND<br>ARMAMENT RSRCH DEV & ENGRG<br>CTR<br>ARMAMENT ENGRG & TECHN LGY<br>CTR<br>ATTN AMSRD AAR AEF T J MATTS<br>BLDG 305<br>ABERDEEN PROVING GROUND MD<br>21005-5001 |
| 1                | US ARMY INFO SYS ENGRG CMND<br>ATTN AMSEL IE TD A RIVERA<br>FT HUACHUCA AZ 85613-5300   |
| 1                | US GOVERNMENT PRINT OFF<br>DEPOSITORY RECEIVING SECTION<br>ATTN MAIL STOP IDAD J TATE<br>732 NORTH CAPITOL ST NW<br>WASHINGTON DC 20402   |

| NO. OF<br>COPIES | ORGANIZATION  |
|------------------|---|
| 22 HCS<br>2 CDS  | US ARMY RSRCH LAB<br>ATTN RDRL VT (ODIR)<br>(1 HCS)<br>ATTN RDRL VTM G MALLICK<br>(10 HCS, 1 CD)<br>BLDG 4603<br>ATTN RDRL WM (A)<br>ATTN RDRL WM S KARNA<br>(10 HCS, 1 CD)<br>BLDG 4600<br>ABERDEEN PROVING GROUND MD<br>21005 |
| 3                | US ARMY RSRCH LAB<br>ATTN IMNE ALC HRR<br>MAIL & RECORDS MGMT<br>ATTN RDRL CIO LL TECHL LIB<br>ATTN RDRL CIO LT TECHL PUB<br>ADELPHI MD 20783-1197  |

TOTAL: 31 (1 ELEC, 2 CDS, 28 HCS)

INTENTIONALLY LEFT BLANK.